Songklanakarin J. Sci. Technol.
33 (5), 585-597, Sep. - Oct. 2011

SJST SONGKLANAKARIN JOURNAL OF SCIENCE AND TECHNOLOGY
http://www.sjst.psu.ac.th

Original Article

Dielectrophoresis of *Tetraselmis* sp., a unicellular green alga, in travelling electric fields analyzed using the RC model for a spheroid

Sakshin Bunthawin[1], Raymond J. Ritchie[1] and Pikul Wanichapichart[2]

[1] *Biotechnology of Electromechanics Research Unit, Faculty of Technology and Environment, Prince of Songkla University, Kathu, Phuket, 83120 Thailand.*

[2] *Membrane Science and Technology Research Centre, Department of Physics, Faculty of Science, Prince of Songkla University, Hat Yai, Songkhla, 90112 Thailand.*

Received 24 May 2011; Accepted 29 August 2011

Abstract

Dielectrophoresis of a unicellular green alga, *Tetraselmis sp.*, in a travelling electric field was analyzed using an RC (resistor-capacitor)-model, instead of the Laplace approach reported in our previous work. The model consists of resistor-capacitor pairs in series to represent the conductive and the capacitive properties of the shell and the inner part of the spheroid. The model is mathematically simpler than the Laplace model and the RC approach is experimentally superior because only the lower critical frequency [LCF] and cell translational speed are required to be measured experimentally. The effective complex impedance of the spheroid was mathematically modeled to obtain the Clausius-Mossotti factor ([CMF]) as a function of cell dielectric properties. Spectra of dielectrophoretic velocity and the lower critical frequency of the marine green alga, *Tetraselmis* sp. were investigated to determine cell dielectric properties using a manual curve-fitting method. Effects of arsenic at different concentrations on the cell were examined to verify the model. Arsenic severely decreases cytoplasmic conductance (σ_c) whereas it increases membrane conductance (σ_m). Effects were easily observable even at the lowest concentration of arsenic used experimentally (1 ppm). The method offers a practical means of manipulating small plant cells and for rapid screening for effects on the dielectric properties of cells of various applied experimental treatments.

Keywords: dielectrophoresis, interdigitated electrodes, phytoplankton, RC model, travelling wave

1. Introduction

Manipulation of cells in travelling electric fields relating two orthogonal linear motions can be used for cell characterization and separation (Wang *et al.*, 1995; Talary *et al.*, 1996; Jones, 2003; Fu *et al.*, 2004). This has great biotechnological potential (Bunthawin *et al.*, 2010). The translational motions of a cell can be termed the dielectrophoretic velocity and is a complex function of the frequency dependent Clausius-Mossotti factor ([CMF]), where the dielectrophoretic spectrum of a spheroidal cell is distinguished from that of a sphere (Bunthawin *et al.*, 2010). Many more biological cells can be approximated by a spheroid than by a simple sphere. The relationship between the real and imaginary parts of the [CMF] reflects boundary frequencies of positive and negative dielectrophoresis; the so-called "critical frequency" (Pohl, 1978; Gimsa *et al.*, 1991; Gimsa and Wachner, 1998; Gimsa and Wachner, 1999; Bunthawin *et al.*, 2007; Bunthawin *et al.*, 2010). In the case of the real part [CMF] (Re[CMF]) prevailing over its imaginary part (Im[CMF]), the spheroid will be either attracted toward the tips or repelled from interdigitated electrodes over AC field frequency ranges from kHz to MHz (Bunthawin *et al.*, 2010). The cell does not move when the imaginary part of the [CMF] predominates.

* Corresponding author.
Email address: sakshin.b@phuket.psu.ac.th

Previously, dielectrophoretic velocity and two critical frequencies of a spheroid in a travelling electric field have been derived through the Laplace approach where the real part of the [CMF] is zero (Gimsa and Wachner, 1998; Gimsa and Wachner, 1999; Bunthawin and Wanichapichart 2007; Bunthawin *et al.*, 2007). Nonetheless, it is evident that the two critical frequencies (high critical frequency, HCF, and low critical frequency, LCF) deduced from such an approach were rather mathematically complicated. Furthermore, a shell thickness of a spheroid simulated from the Laplace approach is non-uniform, the so-called "the confocal shell problem" (Asami *et al.*, 1980; Gimsa and Wachner, 1998, 1999). An RC (resistor-capacitor)-model of a spheroid in a two-phase electric field has thus been proposed by Gimsa and his colleagues (Gimsa *et al.*, 1991; Gimsa and Wachner, 1998) and later extended by Bunthawin *et al.* (2007) and Bunthawin and Wanichapichart (2007) as an impedance approach for a case of a travelling electric field to correct the ambiguities about the shell thickness and the estimated dielectric properties of a spheroidal cells. In the previous RC-model the impedance of the suspension was obtained by Kirchhoffs laws and the "influential radius", a parameter given by the characteristic length to which the field disturbance, was introduced by cell polarization (Gimsa and Wachner, 1998, 1999). The influential radius also concerns the depolarization factor which does not depend on frequency but only on cell geometry (Asami, 2002; Bunthawin and Wanichapichart, 2007).

As reported by Bunthawin and Wanichapichart (2007), the higher critical frequency (HCF) of a marine green phytoplankton alga could not usually be observed experimentally. For this reason, estimations of cell dielectric properties by using a curve-fitting method could not be carried out. The lack of experimental data at HCF raises some doubts about the validity of the estimated cytoplasmic conductivity obtained from such methods (Bunthawin and Wanichapichart, 2007; Bunthawin *et al.*, 2007). Alternatively, the frequency measurement technique can be improved by means of measurement of the dielectrophoretic velocity, which allows one to estimate the cytoplasmic conductivity and permittivity (Bunthawin *et al.*, 2010). In cells undergoing dielectrophoresis in a travelling wave electric field, both positive and negative dielectrophoretic velocities at LCF and HCF are measurable, making it possible to evaluate the dielectric properties of the membrane and the cytoplasm, respectively.

The present study extends the RC model to measurements of dielectrophoretic velocity and critical frequency to determine the dielectric properties of a shelled spheroid in a travelling wave electric field. The RC approach is mathematically simpler than the Laplace model and the RC model is experimentally superior because only the lower critical frequency (LCF) and cell translational speed are required to be measured experimentally. This is a critical advantage over the Laplace model. In this work, the marine green phytoplankton alga *Tetraselmis* sp. is considered to be a single shelled spheroid. The dielectric properties of the cell membrane, cytoplasm and the suspending medium are obtained from manual-curve fitting of the lower critical frequency and cell translational speed. Experimental results from the literature together with the observations of the control and arsenic pre-treated cells are also used to demonstrate the validity of the model. Comparisons will be made to findings in our previous study on yeast cells (Bunthawin *et al.*, 2010).

2. Theoretical Approach

2.1 The critical frequency

Estimates of the two critical frequencies and the dielectrophoretic velocity of a spheroid in a travelling electric field are made based on the concept proposed by Bunthawin *et al.* (2010), where an RC model is employed instead of the Laplace approach. A spheroid with a single shell is assigned an equivalent RC-circuit (Figure 1), using a pair of resistors and capacitors to represent the conductive and the capacitive properties of the shell, the inner part of the spheroid (the cytoplasm) and the suspending medium, respectively. The effective complex impedance of the spheroid is then calculated from the Clausius-Mossotti factor ([CMF]) (Gimsa and Wachner, 1998; 1999). At the boundary frequencies of the positive and the negative dielectrophoresis (DEP), the zero DEP force also relates to the value of the zero-real part of the Clausius-Mossotti factor (Re[CMF]). Two critical frequencies were then solved by using the frequency dependence of Re[CMF] as a function of an angular frequency ($\omega = 2\pi f$). Dielectric dispersion of the spheroid's compartments at lower and higher frequency range is taken into account to extract LCF and HCF from the electric field frequencies (*f*) appearing in Re[CMF]. The modified [CMF] of the RC model is (Gimsa and Wachner, 1999):

$$[\mathrm{CMF}] = \frac{1}{L_k}\left(\frac{U_s^* - U_f^*}{U_s^*}\right), \tag{1}$$

where U_s^* and U_f^* are the electrical potentials of the suspending medium and the cell-medium interface, respectively. The relationship between U_f^* and the specific complex impedances (Z^*) is defined as $U_f^* = \left[\frac{Z_c^* + Z_m^*}{(Z_c^* + Z_m^* + Z_s^*)}\right]\vec{E}.\vec{r}_{\inf}$, where $r_{\inf} = \frac{r}{1-L_k}$ and *r* represents the influential radius or radial distance (see Figure 1). L_k is the depolarization factor which depends on the cell geometry: it has three components along the *x, y,* and *z* axes as L_x, L_y and L_z, respectively. However, for mathematical simplification, the length of the three axes *a*, *b,* and *c* of the spheroid are considered as $a > b = c$, which it is relevant to a shape of *Tetraselmis* sp. (see Figure 2). This analytical case of $b = c$ is a prolate spheroid as proposed by Asami (2002), later extended by Bunthawin *et al.* (2007) and Bunthawin *et al.* (2010). For cell dimensions (see Figures 1 and 2), the ratio $\frac{a}{b} > 1$, $L_k = -\frac{1}{q^2-1} + \frac{q}{(q^2-1)^{3/2}}$

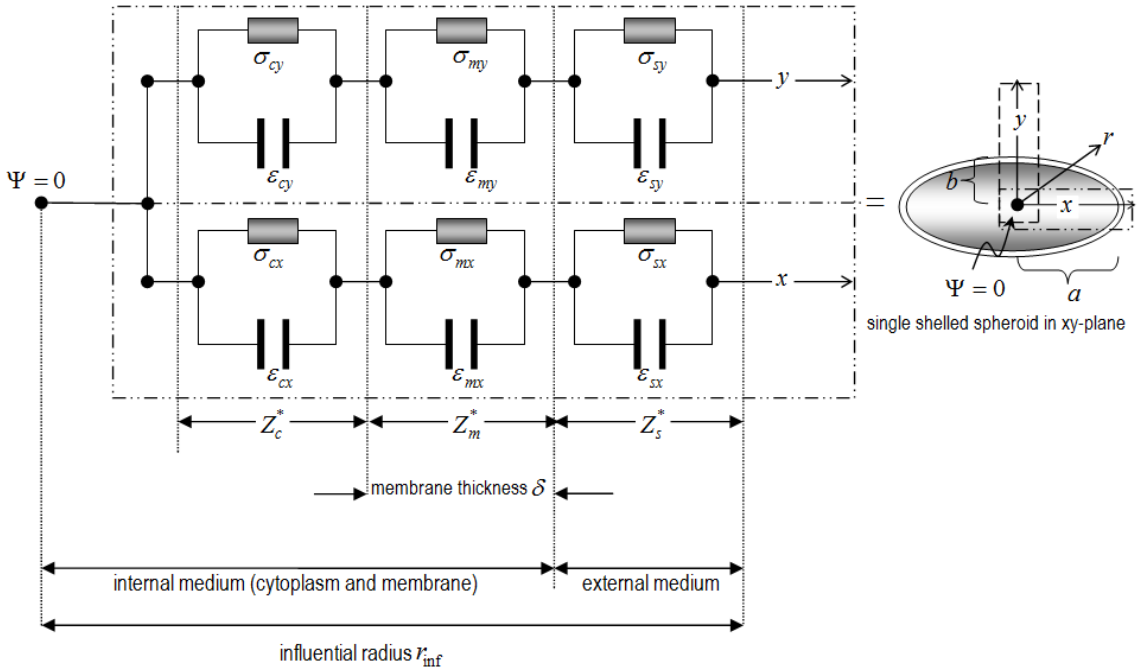

Figure 1. RC model which is equivalent to the shelled polate spheroid (on the right) is shown in *x*- *y* plane with the zero potential ($\psi = 0$) at the center of the spheroid. The conductive and capacitive properties of each branch are represented by their conductivity (σ) and dielectric constant (ε).

$\ell n\left[q+(q^2-1)^{1/2}\right]$, $L_y = L_z = \dfrac{1-L_x}{2}$, and $\sum_k L_k = 1$, where $q = \dfrac{a}{b}$ (Asami *et al* 1980). Combining these expressions, [CMF] along any semi-axis (k) can be written as:

$$[\mathrm{CMF}_k] = \frac{1}{L_k}\left[1 - \frac{Z_c^* + Z_m^*}{(Z_c^* + Z_m^* + Z_s^*)(1-L_k)}\right], \qquad (2)$$

where the specific impedances of the compartments are expressed as (Bunthawin and Wanichapichart, 2007; Bunthawin *et al.*, 2007):

$$Z_{c,m,s}^* = \begin{pmatrix} Z_c^* \\ Z_m^* \\ Z_s^* \end{pmatrix} = \begin{pmatrix} (\sigma_c^*)^{-1} \\ (\sigma_m^*)^{-1} \\ (\sigma_s^*)^{-1} \end{pmatrix} = \begin{pmatrix} (\sigma_c + j\omega\varepsilon_o\varepsilon_c)^{-1} \\ (\sigma_m + j\omega\varepsilon_o\varepsilon_m)^{-1} \\ (\sigma_s + j\omega\varepsilon_o\varepsilon_s)^{-1} \end{pmatrix}. \qquad (3)$$

It should be noted the specific impedances are generally defined as a term of a complex impedance per length (ℓ) and cross section area (A) as the ratio of ℓ / A (Gimsa and Wachner, 1998). Nevertheless, for mathematical tractability,

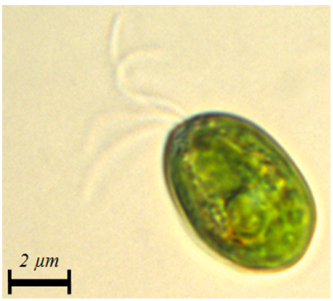

(a)

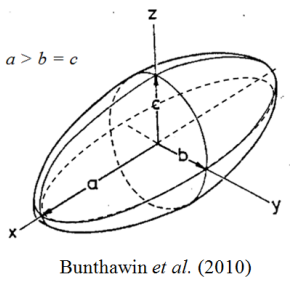

Bunthawin *et al.* (2010)

(b)

Figure 2. Cell of (a) *Tetraselmis* sp. is considered as (b) a single shelled prolate spheroid with average dimension a = 10.0 μm and b = 8.0 μm. Views of isometric (left) represents its three semi-axes along *x*-*y*-*z* plane where $a > b = c$ with a constant shell thickness δ (an averaged value). All axes are measured from the center to the outer surface along their axis.

this ratio is set to be constant throughout this work so that substituting Equation 3 into Equation 2 brings the cancellation of this ratio (Bunthawin *et al.*, 2007 and Bunthawin *et al.*, 2010). The conductive (σ) and capacitive (ε) properties of the cytoplasm (c), the membrane (m) and the suspending medium (s) are assigned as $\sigma_c, \sigma_m, \sigma_s$ and $\varepsilon_c, \varepsilon_m, \varepsilon_s$, respectively, where the permittivity of a vacuum is $\varepsilon_0 = 8.85 \times 10^{-12}$ F.m^{-1} and $j = \sqrt{-1}$. Similarly, three orthogonal components of the $[\mathrm{CMF}_k]$ may be written in tensor forms as:

$$[\mathrm{CMF}_k] = \begin{pmatrix} [\mathrm{CMF}_x] & 0 & 0 \\ 0 & [\mathrm{CMF}_y] & 0 \\ 0 & 0 & [\mathrm{CMF}_z] \end{pmatrix}, \quad (4)$$

with $$L_k = \begin{pmatrix} L_x & 0 & 0 \\ 0 & L_y & 0 \\ 0 & 0 & L_z \end{pmatrix}. \quad (5)$$

Substituting Equation 3 to 5 into Equation 2, for the longest axis in x direction (dielectrophoretic force direction), then

$$[\mathrm{CMF}_x] = \left(\frac{(\sigma_m^* \sigma_s^* + \sigma_c^* \sigma_s^* + \sigma_c^* \sigma_m^*) L_x - \sigma_c^* \sigma_m^*}{\sigma_m^* \sigma_s^* + \sigma_c^* \sigma_s^* + \sigma_c^* \sigma_m^* (L_x^2 - L_x)} \right). \quad (6)$$

The real and imaginary part of the frequency dependence of $[\mathrm{CMF}_x]$ can be solved directly using the relation $[\mathrm{CMF}_x] = \mathrm{Re}[\mathrm{CMF}_x] + j\,\mathrm{Im}[\mathrm{CMF}_x]$. By rearranging Equation 6 in polynomial form of $a_n \omega^n + a_{n-1}\omega^{n-1} + \ldots + a_0 = 0$, where a_n, n are constant and $\omega = 2\pi f$, and setting f = LCF for the lower and f = HCF for the higher critical frequency, then estimates of LCF and HCF are obtained as:

$$\mathrm{HCF} = \frac{\sqrt{-AB}}{2\pi C}, \quad (7)$$

$$\mathrm{LCF} = -\frac{\sqrt{-E(F+G)}}{2\pi D}, \quad (8)$$

where,

$$A = \varepsilon_c(\varepsilon_s \beta - \varepsilon_c - 2\varepsilon_s) + \varepsilon_s^2(\beta - 1),$$

$$B = \beta(\sigma_s^2 + \sigma_c \sigma_s) - 2\sigma_c \sigma_s - (\sigma_c^2 + \sigma_s^2),$$

$$C = \varepsilon_0 A,$$

$$D = \varepsilon_m \varepsilon_0 B,$$

$$E = \beta \sigma_c \sigma_m \sigma_s (2\sigma_s + \sigma_c) - \sigma_c \sigma_s (2\sigma_m^2 + \sigma_c \sigma_s + 2\sigma_m \sigma_s) - \sigma_m^2 \sigma_s^2,$$

$$F = \beta(\sigma_m^2 \sigma_s^2 + \sigma_c^2 \sigma_s^2 + \sigma_c \sigma_s \sigma_m^2) - \sigma_c^2 \sigma_m^2 - 2\sigma_s \sigma_m \sigma_c^2.$$

The final two equations allow one to vary σ_s at arbitrary low values so that HCF and LCF can be measured. When reaches the maximum (critical) value, the two frequencies merge at the zero dielectrophoretic force. Equation 7 and 8 are written in a more compact form and easily to derive than that of Laplace approach (see Appendix A).

2.2 Relation of travelling wave dielectrophoretic force and dielectrophoretic velocity

The time-averaged dielectrophoretic force ($\bar{\bar{F}}_t$) (Wang *et al.*, 1995) acting on a shelled spheroid in a travelling electric field is written in the form (Equation 4, Bunthawin *et al.*, 2010):

$$\bar{\bar{F}}_t = \frac{2}{3}\pi a b^2 \varepsilon_0 \varepsilon_s \left[\mathrm{Re}[\mathrm{CMF}] \nabla E^2 + \mathrm{Im}[\mathrm{CMF}] \left(E_x^2 \nabla \phi_x + E_y^2 \nabla \phi_y + E_z^2 \nabla \phi_z \right) \right] \hat{a}_k \quad (9)$$

where $\hat{a}_k$ (k=x,y,z) are unit vectors in the Cartesian coordinate frame, a and b are semi-axes of the spheroid along the x and y axis, E is the root mean square (rms) value of the electric field strength and ϕ_x, ϕ_y and ϕ_z are the electrical phases addressing the electrode along x, y and z direction, respectively. The magnitude of the conventional force depends on both Re[CMF] and ∇E^2 (gradient of the square of the electric field strength) whereas the direction depends on the sign of the Re[CMF]. In the case of the spheroidal cell travelling with a constant speed through a viscous medium (η), the cell velocity can be written as (Equation 14, Bunthawin *et al.*, 2010):

$$\vec{v}_{cDEP} = \frac{\varepsilon_0 \varepsilon_s b^2 \,\mathrm{Re}[\mathrm{CMF}] \nabla E^2}{9\eta K'} \hat{a}_{\pm x}, \quad (10)$$

where K' is the shape factor that relates with the geometry of the cell (Equation 11, Bunthawin *et al.*, 2010) and $\hat{a}_{\pm x}$ is a unit vector along the x axis. It should be noted that if is negative, the cell will be repelled from the electrode with negative force and the velocity, with reference to the electrode, will be minus.

3. Experimental

3.1 Cell preparation

Cells of *Tetraselmis* sp., obtained from the National Institute for Coastal Aquaculture (NICA), Thailand, were considered as a spheroid with average dimensions a =10.0± 0.7 μm and b = 8.0±0.5 μm (meanSD) (Figure 2). Hence in Figure 1 the long spheroidal axis (a) was taken as 10 mm and the short axis (b) as 8 mm. The cells were cultured in Sato and Serikawa's artificial seawater (Sato and Sarikawa, 1978), and harvested when the cells were in log-growth phase. The cells were centrifuged at 7,000 rpm for 2 min and re-suspended twice in 0.5 M sorbitol solution as described by Wanichapichart *et al.* (2007). The solution conductivity (σ_s) was measured by using a conductivity meter (Tetracon 325, LF 318), and it was adjusted to be between 3 and 300 mS.m^{-1} by adding 0.1 M KCl solution, using a micropipette (Nichipet, model 5000DG). Non-viable cells were prepared by boiling the cells at 80°C for 10 min, cooling down to room temperature, centrifuging and re–suspending in the same experimental solution as was used for the live cells (Wanichapichart *et*

al., 2007). Arsenic pre-treated cells were prepared by adding arsenic solution ($NaAsO_2$, MW 129.9) into the cell culture at concentrations varying from 1 to 150 ppm and leaving them for 24 hrs before being used in an experiment.

3.2 Electrode and electrical setup

Diluted suspensions of cells were used to measure movement in a travelling electric field. About 100 µl of cell suspensions with 9.2×10^6 and 4.0×10^5 cells.ml^{-1} were pipetted onto the glass slide between the electrodes. The interdigitated electrode was fabricated on commercially available standard microscope glass slides of dimension 80301 mm (Marienfeld, Germany). Each bar was made of gold 200 µm in length, 100 µm in width (d_1), and 0.2 µm in thickness (t). The separation of the adjacent bars on the same array (d_2) was 100 µm and that for the central channel (d_3) was 300 µm (Figure 3).

To generate the travelling electric field, the electrode was energized with four sinusoidal signals (a quadrature phase) of 1.4, 2.8, and 7.1 V (rms) in phase sequence as described in Wang *et al.* (1995). A synthesized function generator (Standford Research Systems, Model DS345, California) connecting with a lab-made phase shift unit (PSU) and the inter-junction unit (IJU) was employed to control the phase sequence. As the field frequency of the applied signals was gradually increased, from the lower to the upper limit of the function generator (10 Hz-30 MHz), two critical frequencies LCF and HCF were observed. While cells were undergoing dielectrophoresis, dielectrophoretic velocities ($\vec{v}_{DEP}$) were recorded through CCD camera (Sony SLV-Japan) connecting with a microcomputer (Acer, Aspire 4310). The Winfast PVR™ program was employed to store and display the recording files to determine the velocities using a digital stop-watch function of the Winfast program. Experimental measurements of LCF and HCF and $\vec{v}_{DEP}$ on the cells took

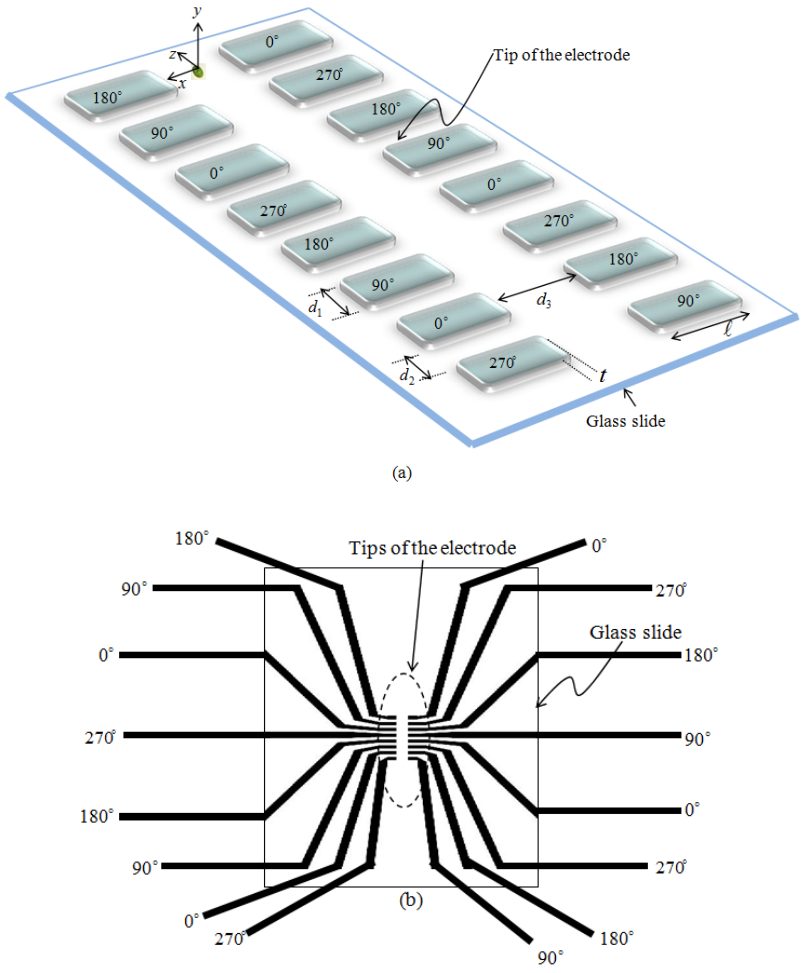

Figure 3. Configuration of the octa-pair interdigitated electrode and the quadrature phase sequence. (a) Three–dimensional view of the electrode tips on the glass slide (not to scale). (b) Diagram of the electrode configuration with exaggerated scale in top view where each bar was made of gold 200 μm in length (ℓ), 100 μm in width (d_1), and 0.2 in thickness (t). The separation of the adjacent bars on the same array (d_2) was 100 and that for the central channel (d_3) was 300.

less than five minutes. Electric field strengths were calculated from the Quick Field™ program version 5.5.

4. Results and Discussion

4.1 The control cells

Suspensions of the control *Tetraselmis* sp. cell (9.2×10^6 and 4.0×10^5 cell.ml^{-1}) subjected to the field strength 28 kV.m^{-1} (equivalent to the signal 1.4 V) underwent positive dielectrophoresis between 50 kHz to 0.5 MHz, where the medium conductivity (σ_s) was ranged from 0.01 to 0.10 S.m^{-1}, respectively (see Figure 4). The theoretical curves were fitted based on *Tetraselmis* cell dimensions a = 10 µm, b = 8 µm and a standard membrane thickness (δ) of 13 nm (Bunthawin *et al.*, 2010). At increasing σ_s (Figure 5a), the magnitudes of the spectra were reduced significantly and the lower critical frequency (LCF) was shifted upwards to a higher frequency. In the case of σ_s = 0.01 S.m^{-1}, the spectrum showed a prominent peak of 9.4 µm.s^{-1} at 200 kHz, where the lower critical frequency was at 50 kHz. For σ_s = 0.03, 0.06, and 0.10 S.m^{-1}, the spectra were transformed into a bell shape with plateaus at heights of 5.2, 4.4, and 3.5 µm.s^{-1}, respectively. The frequency dependency plateaus occupied the range 500 kHz to 10 MHz. The lower critical frequencies (LCF) of the final three σ_s values used were 200, 300, and 500 kHz, respectively.

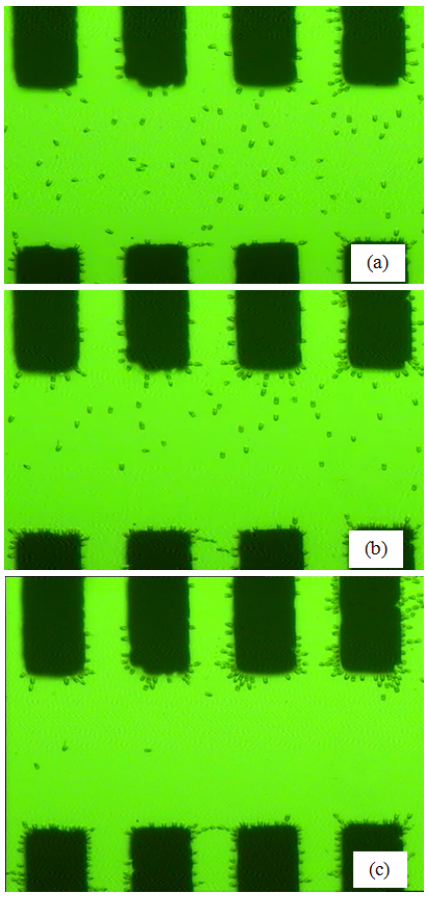

Figure 4. Positive dielectrophoresis induction of *Tetraselmis* sp. in travelling wave electric field for 1.5 min (a-c), using the signal of 50 kHz, 10 Vpp and σ_s = 0.01 S.m^{-1}.

As is seen from Figure 5b, electric field strengths were proportional to the magnitudes of the spectra but did not affect the two critical frequencies. For σ_s = 0.01 S.m^{-1} and 9.2×10^6 cell.ml^{-1}, increasing the field strengths from 28 to 143 kV.m^{-1} brought the peaks up to 29 µm.s^{-1}. For electric field strengths of 28, 57, and 143 kV.m^{-1} the maximum values of the peaks were 9.4, 17.2, and 29.0 µm.s^{-1}, respectively, with all peaks fixed at 300 kHz. However, it is interesting that there were no differences in the dielectrophoretic spectra resulting from using 4.0×10^5 cell.ml^{-1} or 9.2×10^6 cell.ml^{-1} indicating that the technique is not strongly affected by the numerical density of cells used (Figure 5c).

4.2 Arsenic pre-treated and boiled cells

Arsenic had significant effects upon the dielectrophoretic velocity spectra (Figure 6). At increasing concentrations, amplitudes of the spectra and the higher critical frequency were not affected but the lower critical frequency fell in value (Figure 7). Plots of critical frequencies for the control and the arsenic pre-treated cells are shown in Figure 7. It should be noted that electric field strengths did not affect the spectra. For the case of 1, 5, 10, 50, and 150 ppm arsenic pre-treated cells, the lower critical frequencies (LCF) were reduced from 35 kHz to 15 kHz, while the peaks of each spectra remained at the critical conductivity value of 0.25 S.m^{-1}. The spectra for the boiled and the control cells are compared in Figure 8.

4.3 Electrical properties of the cells

As would be predicted from Equation 8 and the real part of the [CMF] in Equation 10, the lower critical frequency and the dielectrophoretic velocity are solely dependent on the capacitive and conductive properties of the cytoplasm (ε_c, σ_c), the membrane (ε_m, σ_m), and the suspending medium (ε_s, σ_s), respectively. These parameters generally affected different characteristic features of the spectrum. It is clear that the dielectric properties of the membrane relate to the lower critical frequency (LCF) and the magnitude of the negative velocity spectra. For the cytoplasm, its conductivity and permittivity affect the magnitude of the positive velocity and the higher value the HCF value, respectively. Cell size and the membrane thickness will also have effects and so different types of cells would be predicted to behave differently. However, qualitatively the results found for *Tetraselmis* (Table 1) are similar to those we found in yeast (Bunthawin *et al.*, 2010). For example, the cytoplasmic conductivity (σ_c) in both cell types is about 0.3 S m^{-1} and membrane conductivity (σ_m) is about 0.15 µS m^{-1}.

Combination of these sensitivities was employed to evaluate the dielectric properties of the control cells and the

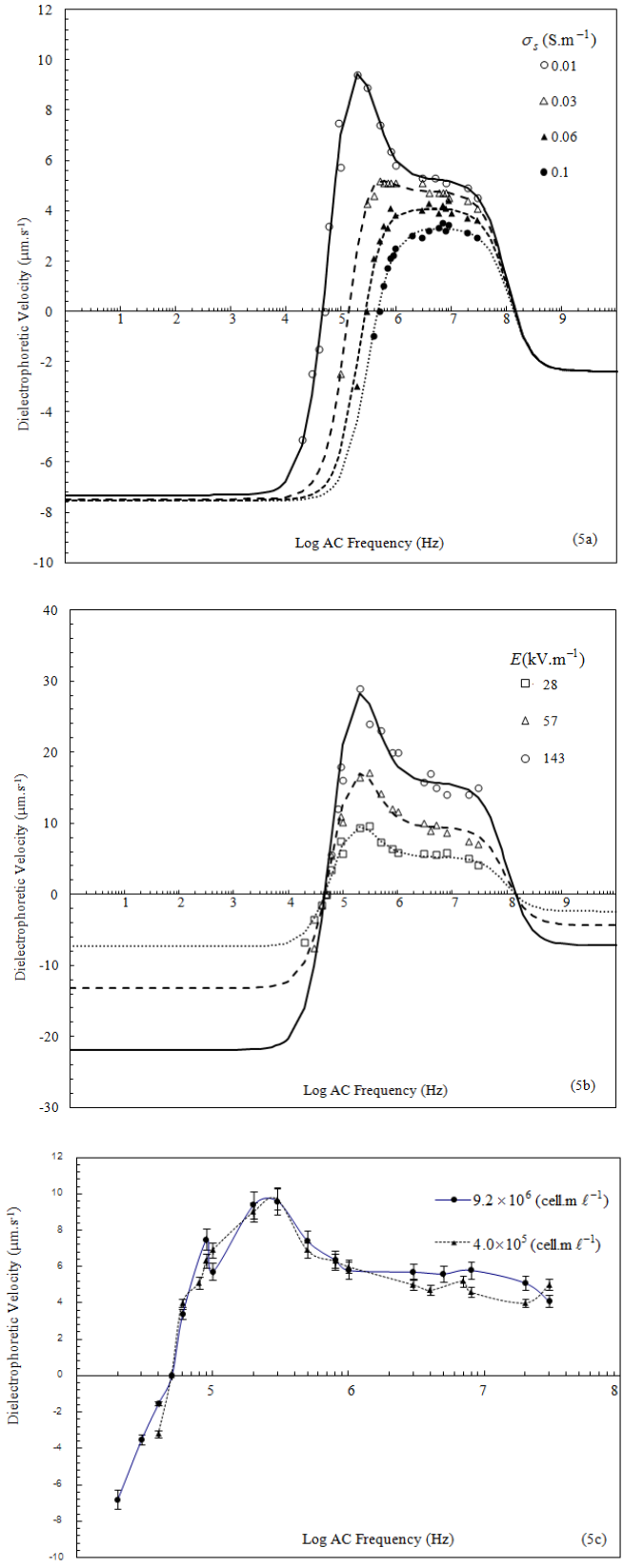

Figure 5. Dielectrophoretic spectrum of the normal cells are affected by (a) the conductivities of the suspending medium (b) the electric field strengths while it is not clearly affected by cell densities (c). Theoretical curves (the solid lines) were plotted by using the dielectric parameters shown in Table 1. The errors in fitting the experimental data to the theoretical expression are less than 10% (Bunthawin *et al.*, 2010).

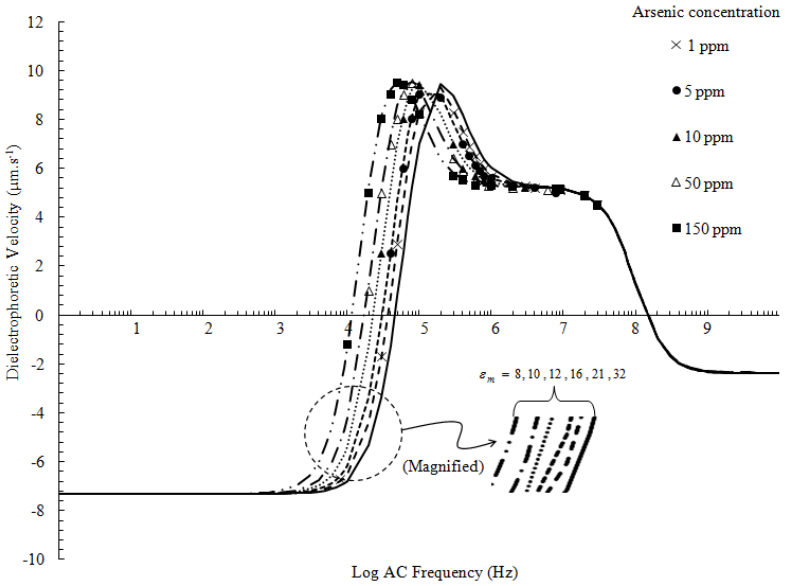

Figure 6. Plots of theoretical and experimental values of dielectrophoretic velocity as a function of field frequency. The theoretical lines were plotted using the following parameters: $\sigma_s = 0.01$ S.m^{-1}, $\sigma_m = 3\times10^{-6}$ S.m^{-1}, $\sigma_c =$ 0.37 S.m^{-1}, $\varepsilon_c = 48$, $\varepsilon_s = 78$, a = 10, $b = c = 8$ μm, and $\delta = 13$ nm.

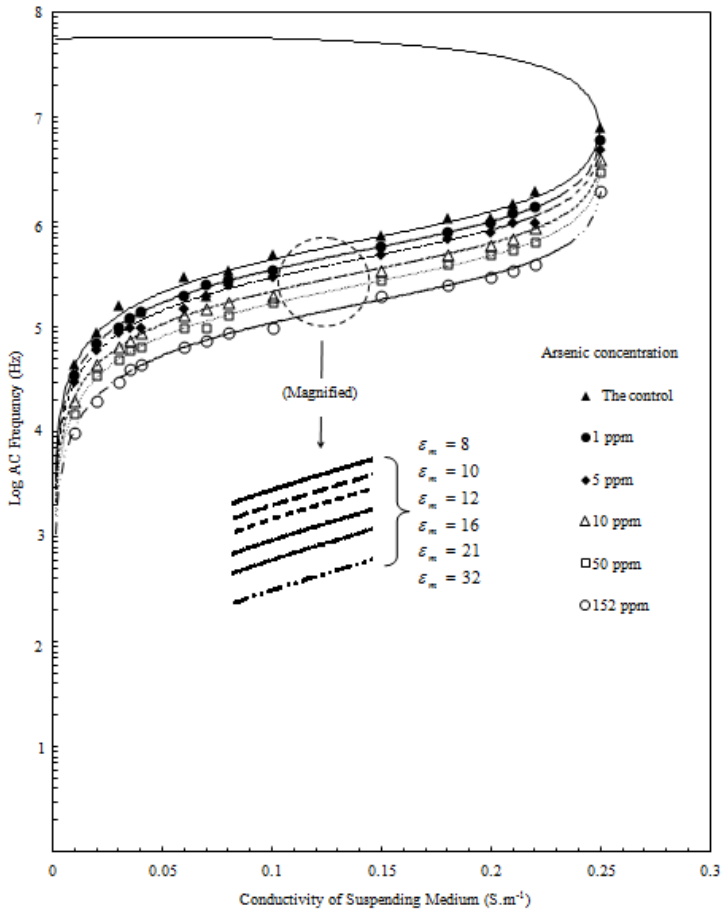

Figure 7. Effect of concentrations of arsenic solution on the lower critical frequency spectra of the arsenic pretreated cells compared with the normal cells. Experimental data (dots) were obtained from cell suspensions subjected to field strength of 28 kV.m^{-1}. Theoretical curves (lines) were simulated by using the dielectric parameters in Table 1.

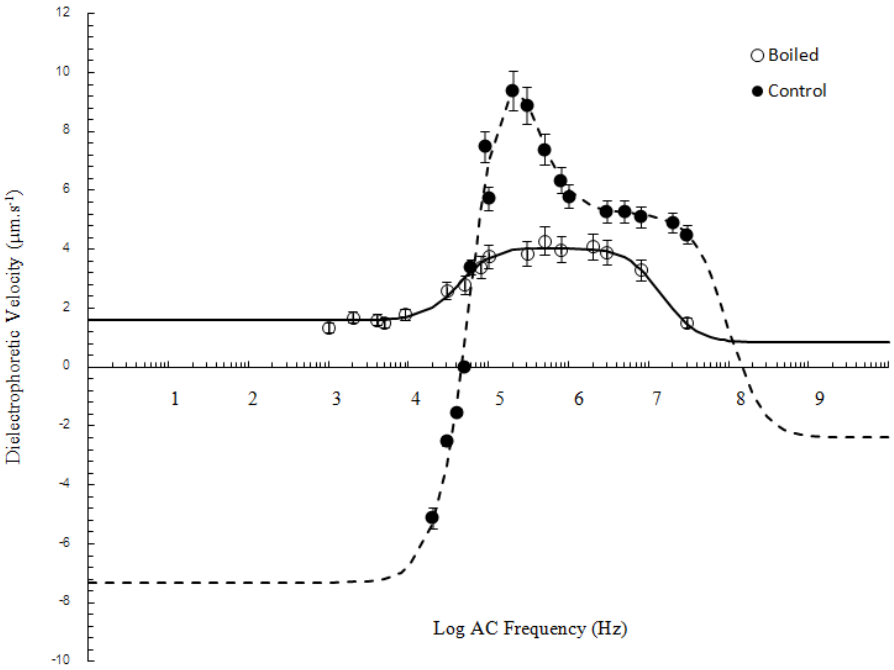

Figure 8. Plot of the dielectrophoretic spectrum of the boiled cells as compared with the control cells. Theoretical curves (the solid and interrupt lines) were plotted by using the dielectric parameters as shown in Table 1.

Table 1. Summary of the conductivities and dielectric constants of the cytoplasm, the cell membrane, and the suspending medium for normal and arsenic pre-treated cells.

Parameters	Control	As pre-treated (ppm)					Boiled cells
		1	5	10	50	150	
σ_c $(S.m^{-1})$	0.37	0.030	0.030	0.028	0.025	0.013	0.06
σ_m $(\mu S.m^{-1})$	0.17	3.0	3.1	3.4	3.7	3.8	30
$\varepsilon_c(F.m^{-1})$	48	48	48	48	48	48	91
$\varepsilon_m(F.m^{-1})$	8	10	12	16	21	32	20
$\varepsilon_s(F.m^{-1})$	78	78	78	78	78	78	78
Cell dimension (Fig. 1) a (μm)	10	10	10	10	10	10	10
Cell dimension (Fig. 1) $b = c$ (μm)	8	8	8	8	8	8	8
Membrane thickness δ (nm)	13	13	13	13	13	13	13

arsenic pre-treated cells (Table 1). Arsenic was found to severely affect both the conductance of both the cytoplasm and cell membrane (σ_c and σ_m) but arsenic decreases σ_c whereas it increases σ_m. Effects are easily observable even at the lowest concentration of arsenic used experimentally (1 ppm), suggesting that arsenic poisoning of cells could be detectable at very low concentrations using the technique.

5. Conclusion

This study proposes the complete RC-model representing a spheroidal cell in a travelling electric field as a solution to the confocal shell problem for a spheroid, i.e. a layer of non-constant thickness can be applied as well to unicellular algal cells as it can to yeast (Bunthawin *et al.*, 2010). The model consists of three resistor-capacitor pairs describing the conductive and capacitive of the cytoplasm, the cell membrane and the suspending solution with no approximations being necessary. To describe a cell translation in a travelling electric field, the dielectrophoretic velocity and two critical frequencies (LCF and HCF) were identified. Both are expressed in terms of the real part of the Clausius-Mossotti factor, which is used to describe cell dielectric properties.

The RC approach provides a simpler to apply model for biological cells compared with the Laplace approach (see Appendix A) because only the lower critical frequency [LCF] and cell translational speed are required to be measured ex-

perimentally. This is a critical advantage over the Laplace approach (Gimsa and Wachner, 1998 and 1999; Bunthawin and Wanichapichart, 2007; Bunthawin *et al.*, 2007) because the lower critical frequency [LCF] and translational speeds are easily measured experimentally on living cells, the high critical frequency [HCF] is often not measureable on cells. By increasing the solution conductivity (σ_s), two frequencies converge and join as soon as the σ_s reaches a critical value (σ_{ct}). Under this critical conductivity the cell experiences a zero force, and the conductivity of the cytoplasm (σ_c) can be predicted. The RC model allowed the evaluation of permittivity and conductivity of the membrane and the cytoplasm of control and arsenic pre-treated cells. Since significant differences could be detected between control and arsenic treated cells the RC model offers the possibility that dielectrophoretic methods could be used for separation of different types of cells or even cells differing in metabolic status such as successfully fertilized cells from non viable egg cells in IVF programs and cancerous from normal cells and for screening cells such as genetically modified plant protoplasts in biotechnological applications. We found experimentally that the numerical density of the cells in the cell suspension does not appear to be critical. This observation has important implications for practical applications of the technique.

Acknowledgements

This work was partially supported by Faculty of Technology and Environment (TE) and Prince of Songkla University (PSU), Thailand, through Biotechnology of Electromechanics Research Unit. Thanks are also extended to NICA for providing the *Tetraselmis* sp. cell cultures and A. Tuantranont and his colleges (MEMS-NECTEC) for supporting the microelectrode array.

References

Asami, K., Hanai, T. and Koizumi, N. 1980. Dielectric approach to suspensions of ellipsoidal particles covered with a shell in particular reference to biological cells. Japanese Journal of Applied Physics. 19, 359-365.

Asami, K. 2002. Characterization of biological cells by dielectric spectroscopy. Non-Crystal Solids. 305, 268-277.

Bunthawin, S. and Wanichapichart, P. 2007. An RC-model for dielectrophoresis of ellipsoidal cells: A method for determination of dielectric properties. Proceeding of the 2nd IEEE International Conference on Nano/Micro Engineering and Molecular Systems, Bangkok, Thailand, January 16-19, 2007, 472-477.

Bunthawin, S., Wanichapichart, P. and Gimsa, J. 2007. An investigation of dielectric properties of biological cells using RC-model. Songklanakarin Journal of Science and Technology. 29 (4), 1163-1181.

Bunthawin, S., Wanichapichart, P., Tuantranont, A. and Coster, H.G.L. 2010. Dielectrophoretic spectra of translational velocity and critical frequency for a spheroid in travelling electric field. Biomicrofluidics. 4:014102 [doi:10.1063/1.3294082].

Fu, L.M., Lee, G.B., Lin, Y.H. and Yang, R.J. 2004. Manipulation of microparticles using new modes of travelling wave dielectrophoretic force: Numerical simulation and experiments. Journal of IEEE/ASME Transactions (Mechatronics). 9 (2), 377-383.

Gimsa, J., Marszalek, P., Loewe, U. and Tsong, T.Y. 1991. Dielectrophoresis and electrorotation of *Neurospora* slime and marine myeloma cells. Biophysical Journal. 60, 749-760.

Gimsa, J. and Wachner, D. 1998. A unified resistor-capacitor model for impedance, dielectrophoresis, electrorotation and induced transmembrane potential. Biophysical Journal. 75, 1107-1116.

Gimsa, J. and Wachner, D. 1999. A polarization model overcoming the geometric restrictions of the Laplace solution for spheroidal cells: Obtaining new equations for field-induced forces and transmembrane potential. Biophysical Journal. 77, 1316-1326.

Jones, T.B. 2003. Basic theory of dielectrophoresis and electrorotation. IEEE Engineering in Medicine and Biology Magazine. 22(6), 33-42.

Landau, L. D. and Liftschitz, E.M. 1985. Elektrodanamik der Kontinua, Akademie-Verlag, Berlin, volume 8.

Pohl, H.A. 1978. Dielectrophoresis: the behaviour of neutral matter in non-uniform electric fields. Cambridge Press, Cambridge, U.K., pp. 214-216.

Sato, T. and Sarikawa, M. 1978. Mass culture of a marine diatom, *Nitzchia closterium*. Bulletin of Plankton Society of Japan. 15 (1), 13-16.

Schwan, H. P. 1988. Dielectric spectroscopy and electro-rotation of biological cells. Journal of Ferroelectrics. 86, 205-223.

Talary, M.S., Burt, J.P.H., Tame, J.A. and Pethig R.J. 1996. Electromanipulation and separation of cells using travelling electric fields. Journal of Physics D: Applied Physics. 29, 2198-2203.

Wang, X.B., Hughes, M.P., Huang, Y., Becker, F.F. and Gascoyne, P.R.C. 1995. Non-uniform spatial distributions of both the magnitude and phase of AC electric fields determine dielectrophoretic forces. Biochimica et Biophysica Acta. 1243, 185-194.

Wanichapichart, P., Wongluksanapan, T. and Khooburat, L. 2007. Electrorotation: diagnostic tool for abnormality of marine phytoplankton cells. Proceedings of the 2nd IEEE International Conference on Nano/Micro Engineering and Molecular Systems, Bangkok, Thailand, January 16 - 19, 2007, 1115-1120.

Abbreviations

a, long spheroidal cell axis (mm);
b, short spheroidal cell axis (mm);
δ, membrane thickness (nm);
[CMF], Clausius-Mossotti Factor;
Re[CMF], real part of C-M factor;
Im[CMF] imaginary part of C-M factor;
[HCF], High Critical Frequency;
[LCF], Low Critical Frequency;
L_k is the depolarization factor which has three components on axes x, y & z (L_x, L_y & L_z);
RC-model, Resistor-Capacitor model;
σ_c electrical conductance of the cytoplasm;
σ_m conductance of the cell membrane;
σ_s conductance of the suspending medium; capacitive and conductive properties of the cytoplasm ($\varepsilon_c, \varepsilon_m, \varepsilon_s$), capacitance of membrane, cytoplasm and external medium respectively.

Appendix (A)

Two critical frequencies of Laplace approach

The effective complex dielectric of a homogeneous spheroid is defined as (Asami *et al.*, 1980)

$$\varepsilon^*_{eff} = \varepsilon^*_m \left(\frac{\varepsilon^*_m + (\varepsilon^*_c - \varepsilon^*_m)\left(L_k + v(1-L_k)\right)}{\varepsilon^*_m + (\varepsilon^*_c - \varepsilon^*_m)\left(L_k + (1-v)\right)} \right), \quad \text{(A1)}$$

where $k = x, y, z$ and $v = \left(1-\frac{\delta}{a}\right)\left(1-\frac{\delta}{b}\right)^2$. The complex dielectrics of cytoplasm, membrane and suspending medium are defined as $\varepsilon_c^* = \varepsilon_c - j\frac{\sigma_c}{\omega\varepsilon_o}$, $\varepsilon_m^* = \varepsilon_m - j\frac{\sigma_m}{\omega\varepsilon_o}$ and $\varepsilon_s^* = \varepsilon_s - j\frac{\sigma_s}{\omega\varepsilon_o}$, respectively. Substituting these complex forms into Equation A1 yields

$$\varepsilon^*_{eff} = (\varepsilon_m - j\frac{\sigma_m}{\omega\varepsilon_0}) \left(\frac{(\varepsilon_m - j\frac{\sigma_m}{\omega\varepsilon_0}) + (\varepsilon_c - \varepsilon_m + j\frac{\sigma_c - \sigma_m}{\omega\varepsilon_0})\left(L_k + v(1-L_k)\right)}{(\varepsilon_m - j\frac{\sigma_m}{\omega\varepsilon_0}) + (\varepsilon_c - \varepsilon_m + j\frac{\sigma_c - \sigma_m}{\omega\varepsilon_0})\left(L_k + (1-v)\right)} \right), \quad \text{(A2)}$$

where its real and imaginary parts are

$$\mathrm{Re}[\varepsilon^*_{eff}] = \frac{1}{\omega\varepsilon_0}\left(\frac{\left(\omega^2\varepsilon_0^2\varepsilon_m A + \sigma_m B\right)\left(\omega\varepsilon_0 C\right) + \omega\varepsilon_0 D\left(\varepsilon_m B - \sigma_m A\right)}{\left(\omega\varepsilon_0 C\right)^2 + D^2} \right), \quad \text{(A3)}$$

$$\mathrm{Im}[\varepsilon^*_{eff}] = \frac{1}{\omega\varepsilon_0}\left(\frac{\omega^2\varepsilon_0^2 C\left(\varepsilon_m B - \sigma_m A\right) - D\left(\omega^2\varepsilon_0^2\varepsilon_m A + \sigma_m B\right)}{\left(\omega\varepsilon_0 C\right)^2 + D^2} \right). \quad \text{(A4)}$$

The constants A, B, C and D stand for

$$A = \varepsilon_m + \alpha(\varepsilon_c - \varepsilon_m),$$
$$B = \alpha(\sigma_m - \sigma_c) - \sigma_m,$$
$$C = \varepsilon_m + \beta b(\varepsilon_c - \varepsilon_m),$$
$$D = \beta(\sigma_m - \sigma_c) - \sigma_m,$$

where $\alpha = L_k + v(1-L_k)$, $\beta = L_k(1-v)$.

Landua and Lifschitz (1985) defined the Clausius-Mossotti factor ([CMF]) as $[\mathrm{CMF}] = \dfrac{\varepsilon^*_{eff} - \varepsilon^*_s}{\varepsilon^*_s + (\varepsilon^*_{eff} - \varepsilon^*_s)L_k}$. For a spheroid with the volume of $V = \dfrac{4}{3}\pi ab^2$ (a case of *Tetraselmis* sp.), the real and the imaginary parts of the [CMF] are then expressed as

$$\mathrm{Re}[\mathrm{CMF}] = [(\frac{A_1A_3 + A_2A_4}{A_3^{\,2} + A_4^{\,2}})], \tag{A5}$$

$$\mathrm{Im}[\mathrm{CMF}] = [(\frac{A_1A_3 - A_2A_4}{A_3^{\,2} + A_4^{\,2}})], \tag{A6}$$

where

$$A_1 = \mathrm{Re}[\varepsilon^*_{eff}] - \omega\varepsilon_0\varepsilon_s,$$
$$A_2 = \mathrm{Im}[\varepsilon^*_{eff}] - \sigma_s,$$
$$A_3 = \omega\varepsilon_0\varepsilon_s(1 - L_k) + \mathrm{Re}[\varepsilon^*_{eff}]L_k,$$
$$A_4 = \mathrm{Im}[\varepsilon^*_{eff}]L_k - \sigma_s(L_k + 1),$$

with $\varepsilon_0 = 8.85\times10^{-12}$ F.m^{-1}, $\omega = 2\pi f$ (rad.s^{-1}), f in Hertz $\mathrm{Re}[\varepsilon^*_{eff}]$ and and the $\mathrm{Im}[\varepsilon^*_{eff}]$ are from Equation A3 and **A4**, respectively.

To obtain an express for two critical frequencies via Equation A5 and A6 are quite complex. The lower [LCF] and the higher [HCF] critical frequencies of the model can, however, be separately derived from the condition Re[CMF]=0. Approximations are made by using the principle of dielectric dispersion of a cell as suggested by Schwan (1988), i.e. the dielectric properties of the cell membrane are prominent in the lower frequencies range (α, β dispersions). The complex dielectric form of each compartment becomes

$$\varepsilon_c^{\,*} \approx -j\frac{\sigma_c}{\omega\varepsilon_o} \text{ and } \sigma_c^{\,*} \approx \sigma_c, \tag{A7}$$

$$\varepsilon_m^{\,*} = \varepsilon_m - j\frac{\sigma_m}{\omega\varepsilon_o} \text{ and } \sigma_m^{\,*} = \sigma_m + j\omega\varepsilon_m\varepsilon_o, \tag{A8}$$

$$\varepsilon_s^{\,*} \approx -j\frac{\sigma_s}{\omega\varepsilon_o} \text{ and } \sigma_s^{\,*} \approx \sigma_s. \tag{A9}$$

On the other hand, those of the cytoplasm are dominant in the higher frequency range providing

$$\varepsilon_c^{\,*} = \varepsilon_c - j\frac{\sigma_c}{\omega\varepsilon_o} \text{ and } \sigma_c^{\,*} = \sigma_c + j\omega\varepsilon_c\varepsilon_o, \tag{A10}$$

$$\varepsilon_m^{\,*} \approx \varepsilon_m \text{ and } \sigma_m^{\,*} = 0, \tag{A11}$$

$$\varepsilon_s^{\,*} = \varepsilon_s - j\frac{\sigma_s}{\omega\varepsilon_o} \text{ and } \sigma_s^{\,*} = \sigma_s + j\omega\varepsilon_s\varepsilon_o. \tag{A12}$$

Substituting Equation A7 to A9 and A10 to A12 to Equation A5 yields the angular frequency (ω) dependence of the Re[CMF] for [LCF] and [HCF], respectively. For the lower case, the Re[CMF] is expressed as

$$\mathrm{Re}[\mathrm{CMF}]_{low} = \frac{\omega^2 Z_1'Z_3' + (\omega Z_2' + \sigma_s)(\omega Z_4' + Z_5')}{\omega^2 Z_3'^2 + (\omega Z_4' + Z_5')^2}, \tag{A13}$$

where

$$Z_1' = \varepsilon_0 \,\mathrm{Re}[\varepsilon^*_{eff(\ell ow)}],$$
$$Z_2^* = \varepsilon_0 \,\mathrm{Im}[\varepsilon^*_{eff(\ell ow)}],$$
$$Z_3^* = \varepsilon_0 L_k \,\mathrm{Re}[\varepsilon^*_{eff(\ell ow)}],$$
$$Z_4^* = \varepsilon_0 L_k \,\mathrm{Im}[\varepsilon^*_{eff(\ell ow)}],$$
$$Z_5^* = L_k(\sigma_s - 1),$$

and

$$\mathrm{Re}[\varepsilon^*_{eff(\ell ow)}] = \frac{\omega^2 Z_6' Z_7' + Z_8' Z_9'}{\omega^2 Z_7'^2 + Z_9'^2}, \tag{A14}$$

$$\mathrm{Im}[\varepsilon^*_{eff(\ell ow)}] = \frac{\omega(Z_6' Z_9' - Z_7' Z_8')}{\omega^2 Z_7'^2 + Z_9'^2}, \tag{A15}$$

where

$$Z_6' = \varepsilon_0[\varepsilon_m^2 + a'\varepsilon_m(\varepsilon_c - \varepsilon_m)],$$
$$Z_7^* = \varepsilon_0[\varepsilon_m + b'(\varepsilon_c - \varepsilon_m)],$$
$$Z_8^* = a'\varepsilon_m\sigma_c,$$
$$Z_9^* = b'\sigma_c,$$

with $a' = L_k + v(1-L_k)$, $b' = L_k(1-v)$, $v = \left(1-\frac{\delta}{a}\right)\left(1-\frac{\delta}{b}\right)^2$.

Setting Eq. (A13) = 0 and then solving for ω, yields the functions

$$\omega_{\ell ow} = \frac{1}{2\varepsilon_0 Z_6'}\sqrt{-\frac{1}{L_k}\left(\alpha_1 - 2\sqrt{\alpha_2 + \alpha_3}\right)}, \tag{A16}$$

since $\omega_{\ell ow} = 2\pi[\mathrm{LCF}]$, then

$$[\mathrm{LCF}] = \frac{1}{4\pi\varepsilon_0 Z_6'}\sqrt{-\frac{1}{L_k}\left(\alpha_1 - 2\sqrt{\alpha_2 + \alpha_3}\right)}, \tag{A17}$$

where

$$\alpha_1 = 2\varepsilon_0\sigma_s Z_7' Z_8'(1-2L_k) - 2Z_7'^2\sigma_s^2(1-L_k) - 2\varepsilon_0\sigma_s Z_6' Z_9'(1-2L_k) - 2\varepsilon_0^2 L_k,$$
$$\alpha_2 = \varepsilon_0^2\sigma_s^2\left(Z_7'^2(6L_k-1) - 2Z_6' Z_7' Z_8' Z_9'\right) + 2\varepsilon_0^3\sigma_s L_k Z_6' Z_9'(1-2L_k) +$$
$$Z_7'^4\sigma_s^4 L_k(L_k-2) - 2\varepsilon_0\sigma_s^3 Z_7'^3 Z_8'(2L_k^2+1) + 4\varepsilon_0^3\sigma_s Z_7' Z_8' L_k^2,$$
$$\alpha_3 = 6\varepsilon_0\sigma_s^2 L_k Z_7'^2\left(Z_7' Z_8'\sigma_s - \varepsilon_0 L_k\right) + 8\sigma_s^2\varepsilon_0^2 L_k Z_6' Z_7' Z_8' Z_9'(1-L_k) +$$
$$2\varepsilon_0\sigma_s Z_7'(Z_6' Z_7' Z_9'\sigma_s^2 - \varepsilon_0 Z_8' L_k) + 2\varepsilon_0 Z_7'^2\sigma_s^3 Z_6' Z_9' L_k(2L_k-3) +$$
$$\varepsilon_0^2\sigma_s^2(Z_6' Z_9')^2 L_k^2 + Z_7'^2\sigma_s^4 + \varepsilon_0^4 L_k^2.$$

A similar procedure was applied for the higher critical frequency, yielding

$$[\mathrm{HCF}] = \frac{1}{4\pi\varepsilon_0 Z_6'}\sqrt{\frac{1}{L_k}\left(\alpha_1 + 2\sqrt{\alpha_2 + \alpha_3}\right)}. \tag{A18}$$

Theoretical plots of the lower and the higher critical frequencies are the same result as the RC-model but the latter is more easily to derive.